CLAS-NOTE 2002-007
CVS: docs/tof_timewalk.tex
Original: May 6, 2002

Systematic Study of Time-walk Corrections for the TOF Counters

by Elton Smith and Rakhsha Nasseripour

1 Background

Time walk is an instrumental shift in the measured time using a leading edge discriminator for the TOF Counters [1]. This time difference is due to the finite rise time of the analog pulse reaching the threshold relative to a reference time. This effect can be minimized in hardware by using constant-fraction discriminators, or by making software corrections to the times using leading-edge discriminators. Historically the measured times, t, produced using leading-edge discriminators have been corrected for the size of the pulse using the measured pulse integral, or ADC, as follows:

$$t_w = t - f_w(x) + f_w(x_{ref}), \tag{1}$$

where t_w is the walk-corrected time, and f_w is the time-walk correction function, which is a function of the measured ADC of the pulse relative to the discriminator threshold (x). In general only time differences of a system are important, so the time-walk correction is specified relative to a time at an arbitrary but fixed pulse height (x_{ref}). We take this point to be the nominal energy-loss peak of minimum ionizing particles, which corresponds to a typical energy loss for our scintillating counters. This type of correction assumes that the shape of the pulses are independent of pulse height. The traditional correction function which has been used (see for example

[2, 3]) is

$$f_w(x) = w_1 + \frac{w_2}{\sqrt{x}} \tag{2}$$

where w_1 and w_2 are determined to optimize the time resolution of the system. The constant w_1 cancels when the correction is made (see Eq. (1)), but is often needed in the fitting procedure itself.

The traditional form for the time-walk correction function (Eq. (2)) does not adequately describe the behavior of pulses over a large dynamical range (see for example Ref. [4]), so more general forms have been used to optimize the time resolution of scintillator time-of-flight systems. After studying the behavior of several functional forms, we have found a form which has been applied successfully to a large array of scintillator counters used in CEBAF large acceptance detector (CLAS) at Hall B at Jefferson Lab. We study the functional form for the corrections below.

2 Functional Form

The CLAS time-of-flight (TOF) system [5] is a scintillator detector system which consists of six identical sectors. In each sector, there are 48 scintillators with photomultiplier tubes (PMT) at each end. The counters are all 5 cm thick, but vary in lengths from 30 to 430 cm. Therefore the geometry changes considerably throughout the system. We apply the following parameterizations to our time measurements with leading-edge discriminators:

$$t_w = t - f_w\left(\frac{A-P}{Th}\right) + f_w\left(\frac{600}{Th}\right) \tag{3}$$

Where P is the pedestal and TH is the discriminator threshold (20 mV), which corresponds to approximately 35 ADC counts. The peak of the energy loss of minimum-ionizing particles is nominally set to 600 counts by adjusting the PMT high voltage. This form will result $t_w = t$ for minimum-ionizing pulses.

In order to match the time-walk corrections to the required dynamic range, we use a generalized form of Eq. (2) for low pulse heights and a linear term to account for the saturation of the PMT pulses:

$$f_w(x) = w_1 + \frac{w_2}{x^{w_3}} \quad \text{if } x < w_o \tag{4}$$

$$f_w(x) = w_1 + \frac{w_2}{{w_o}^{w_3}}(1 + w_3) - \frac{w_2 w_3}{{w_o}^{w_3+1}}\, x \quad \text{if } x > w_o \tag{5}$$

This parameterization has four constants, (w_1, w_2, w_3 and w_0) which are adjusted for each PMT. The functional form of Eq. (4) is used for the region where $x = \frac{ADC-P}{TH} \leq w_0$ when the PMT pulses begin to saturate. This equation reduces to Eq. (2) when w_3 is equal to 0.5. The form of the time-walk function beyond w_0 is found by assuming a linear form and requiring that both functions and their derivatives be equal at $x = w_0$. As a consequence, the linear behavior is completely determined by the parameters in Eq. (4) once we choose the transition point w_0 in Eq. (5).

The time-walk parameters are obtained for our system by using a laser calibration system which is referenced to the time of a photodiode (see Refs. [5, 6, 7] for details). Times are measured as a function of the pulse height of each PMT using a neutral density filter in front of the laser pulse which feeds each scintillation counter. We determined the parameters of f_w by fitting the measured times as a function of the measured ADC using the laser calibration data for left and right PMTs separately. Fig. 1 shows measured time walk versus ADC channel for one scintillator. The four fit parameters are then put in the CLAS calibration database to be used for time-walk corrections during calibration and reconstruction.

3 Correlated Parameters

The results of the fits which determined the time-walk correction function raised two puzzles. First, the constants varied considerably from counter to counter, even for

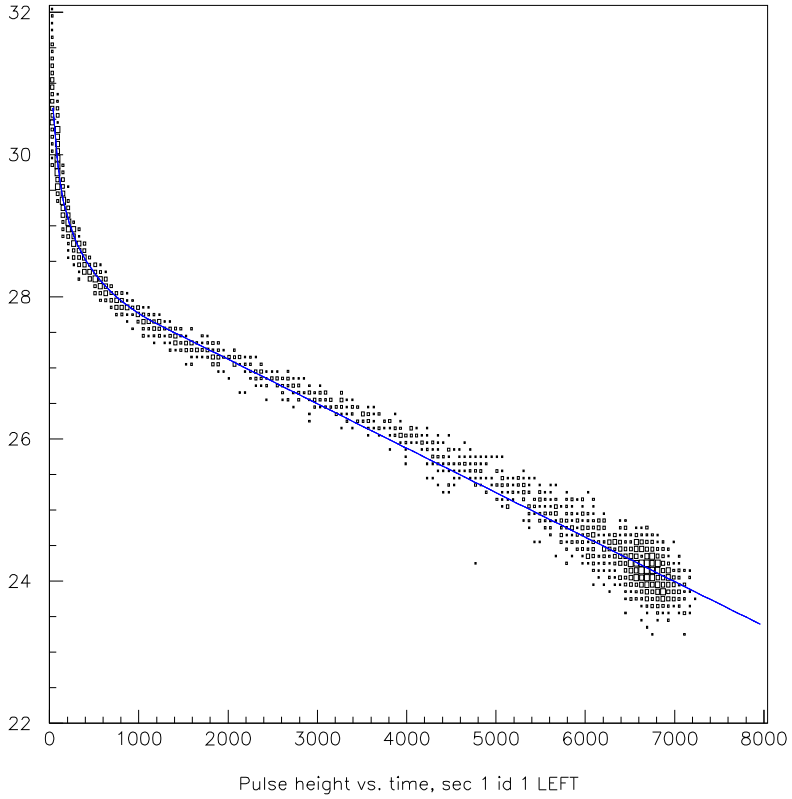

Figure 1: Laser calibration data and the fit function (Eq. (4) and Eq. (5))(sector 1, paddle 1, left PMT).

those of similar construction. Second, the exponent w_3 ranged between zero and 0.5 when we expected a clustering around the one half from Eq. (2). Both puzzles can be understood in light of the strong correlation between w_2 and w_3 which is shown in Fig. 2.

The correlation between the parameters is a reflection of the fact that the time-walk correction functions are not unique, but must have a similar shape in order to adequately describe the data. In order to find the correlation function between w_2 and w_3, we consider the fact that in general a 3-parameter function can be determined uniquely if we specify the function and its first and second derivatives. In the following we do not discuss the constraints arising from the absolute value of the function and drop the parameter w_1 which has no impact on the time-walk correction (see Eq. (3)). Only the shape of the function, determined by the derivatives have a direct effect on the time walk. These conditions can be written in the following way for a function f, which depends explicitly on x and implicitly on two parameters as in Eq. (4):

$$f'(x; w_2, w_3) = f'(x; w_2', w_3') \tag{6}$$

$$f''(x; w_2, w_3) = f''(x; w_2', w_3') \tag{7}$$

The above conditions describe a family of functions, where each member of the family is defined by the pair of parameters w_2' and w_3'. If these conditions were satisfied at all values of x, they would define a single function, and yield $w_2 = w_2'$ and $w_3 = w_3'$. However, the conditions can be satisfied for different values of the parameters at a fixed value of $x = x_0$, while at the same time having first and second derivatives consistent with measured time-walk variations. This introduces a correlation $w_2 = g(w_3)$ between the parameters which we determine by inverting Eq. (6) and (7) and using Eq. (4) at $x = x_0$:

$$w_2 = g(w_3; w_2', w_3', x_0) \equiv \frac{w_2' w_3'}{w_3} \cdot x_0^{(w_3 - w_3')} \tag{8}$$

$$w_2 \;=\; \frac{w_2{}'w_3{}'(w_3{}'+1)}{w_3(w_3+1)} \cdot x_0^{(w_3-w_3{}')} \tag{9}$$

In principle these two constraints could result in substantially different functions, but over the range of interest they are very similar, especially since we take x_0 as a parameter to be determined from data for each counter. Furthermore, the constraint in Eq. (8) using average values for $w_2{}'$, $w_3{}'$ and x_0 does a remarkable job of describing the empirical correlation found in Fig. 2.

4 Functional Form with Constraint

Beyond understanding the correlation between the parameters, a functional form with fewer parameters is often more robust and more likely to be physical. Therefore, we have used our calibration data to determine the best values of $w_2{}'$, $w_3{}'$ and x_0 to construct a reliable time-walk function. The additional constraint can serve as an additional check during the calibration procedure, even in cases where single data points are of dubious quality.

In order to find $w_2{}'$ and $w_3{}'$ and x_0, we used parameters w_2 and w_3 determined from the fitting laser calibration data to the function in Eq. (4) and (5). To increase the quality of the fits in terms of statistics, we group scintillators of similar length into sets of eighteen (three counters per sector and six sectors). The plots shown in Fig. 3 and Fig. 4 are the result of the fits respectively for left and right PMTs. The extracted parameters ($w_2{}'$, $w_3{}'$ and x_0) for each scintillator group are plotted in Fig. 5 (left PMTs) Fig. 6 (right PMTs) versus the average scintillator number for each group. We note that they are almost constant for all scintillators. Therefore, we take the weighted average of each parameter to obtain the correlation function form Eq. (8) for w_2 and w_3 and use it for the entire scintillator system. The computed

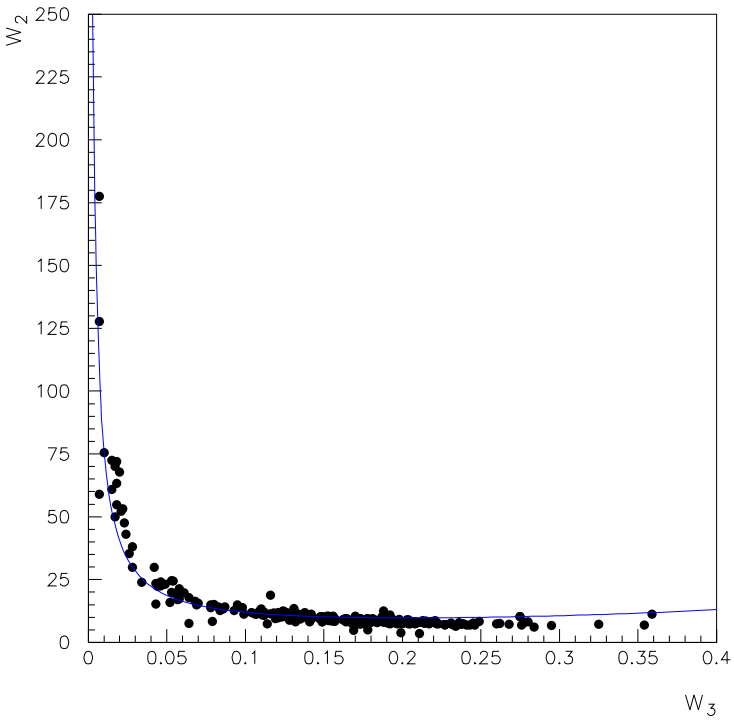

Figure 2: The correlation between the time-walk correction parameters (w_2 versus w_3) determined from fits to the laser data (Eq. (4) and Eq. (5)) is shown for the left PMTs of all 288 TOF scintillators.

average values for the left PMTs are:

$$\begin{aligned} w_2{}' &= 13.9 \pm 0.2 \\ w_3{}' &= 0.08 \pm 0.001 \\ x_0 &= 19.6 \pm 0.3 \end{aligned} \tag{10}$$

Similar values are obtained for the right PMTs (Fig. 6), so we take these values to define the relation between w_2 and w_3 in Eq. (8).

5 Time-walk Correction With The Improved Function

The time-walk function f_w in Eq. (4) and (5) can now be completely specified with three parameters: w_0, w_1 and w_3. The parameter w_2 is computed using the constraint in Eq. (8) with the constants in Eq. (10). We again note that w_1 cancels out when computing the time-walk correction, so the parameterization has only two effective parameters. Using this algorithm, the TOF laser data in run 31154 were refit for w_0, w_1 and w_3 and the corresponding w_2 by computation. The parameters determined in this way are compared to the fit allowing all four parameters to float in Figures 7 and 8. The results are given separately for the left and right PMTs. We note that the constrained fit results in smaller variation of the parameter w_0 over all scintillators, and results in slightly larger values of w_3 away from the singularity at zero.

We checked the consistency of the behavior of the fitted parameters by comparing the results for the left and right PMTs, which should be similar by construction. The parameters are shown in Fig. 9. Indeed, the results are strongly correlated. In addition we find that by applying one more constraint, and therefore having one less parameter, we have actually improved the χ^2 per degree of freedom of the fit (see

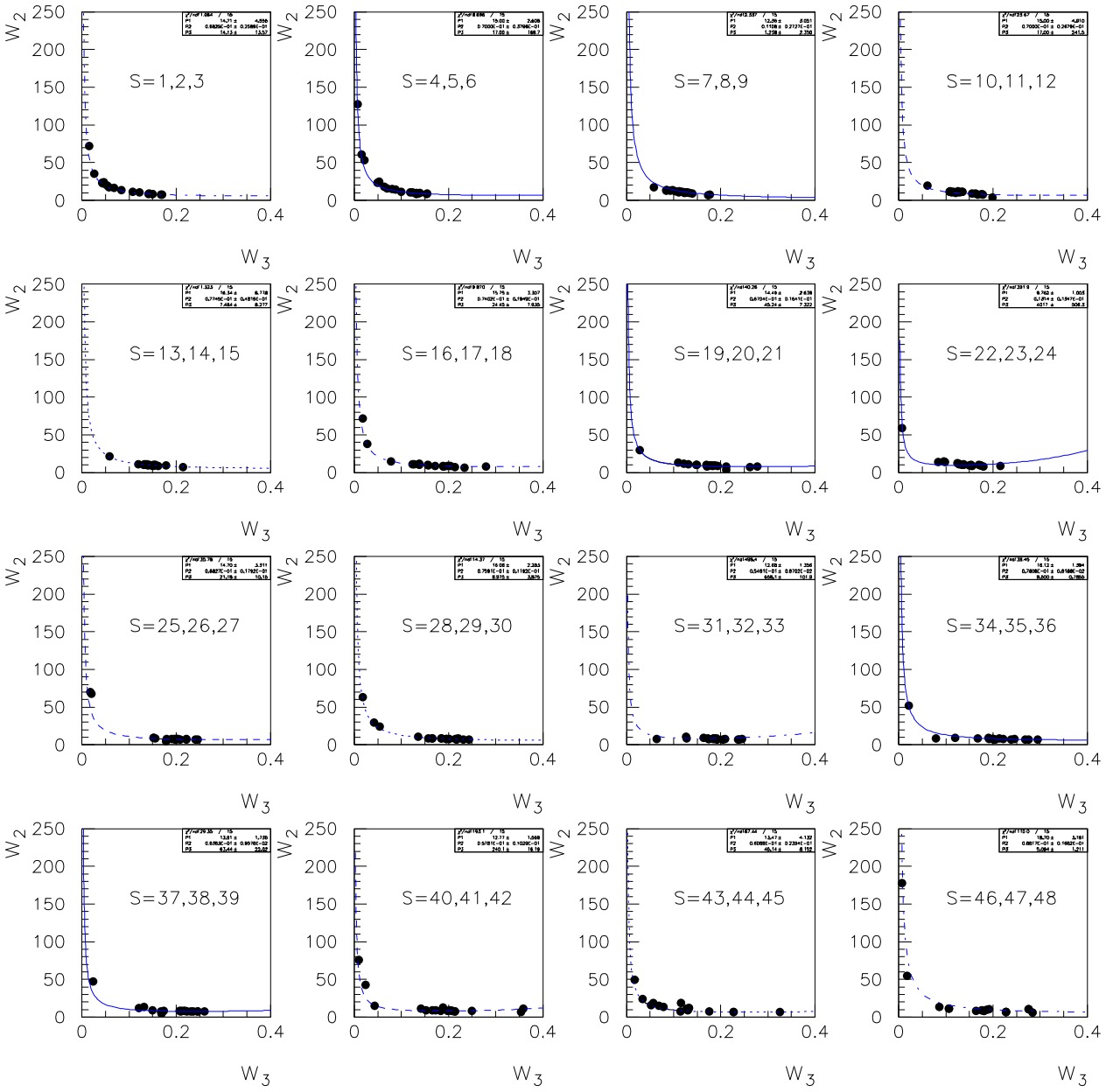

Figure 3: The fitted parameters w_2 and w_3 are plotted in group of 3 scintillators for all six sectors (left PMTs). The scintillators are specified on the plots. The fit $w_2 = g(w_3; w_2', w_3', x_0)$ (Eq. 8) determines w_2', w_3' and x_0 for each group of scintillators.

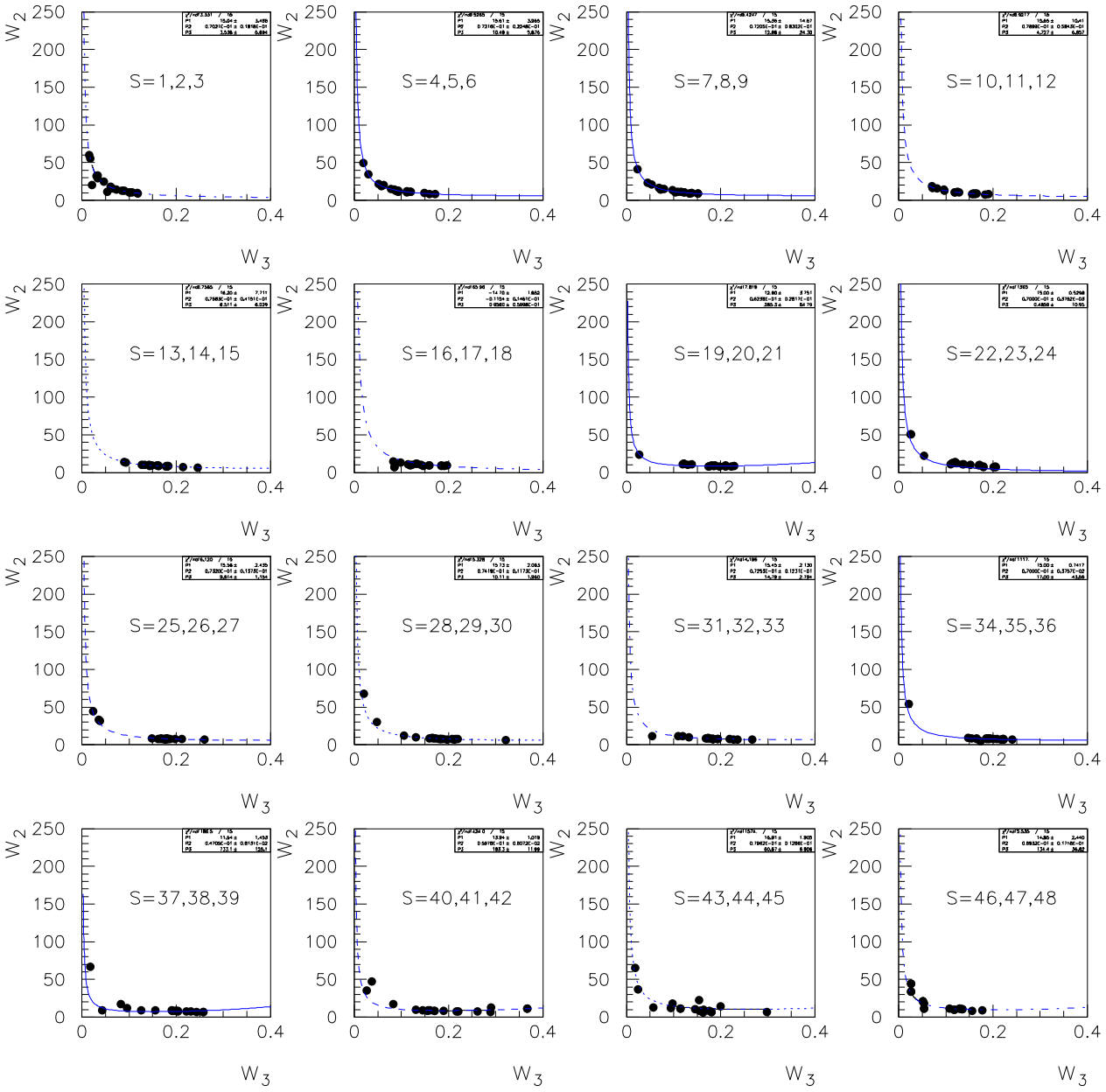

Figure 4: The fitted parameters w_2 and w_3 are plotted in group of 3 scintillators for all six sectors (right PMTs). The scintillators are specified on the plots. The fit $w_2 = g(w_3; w_2', w_3', x_0)$ (Eq. 8) determines w_2', w_3' and x_0 for each group of scintillators.

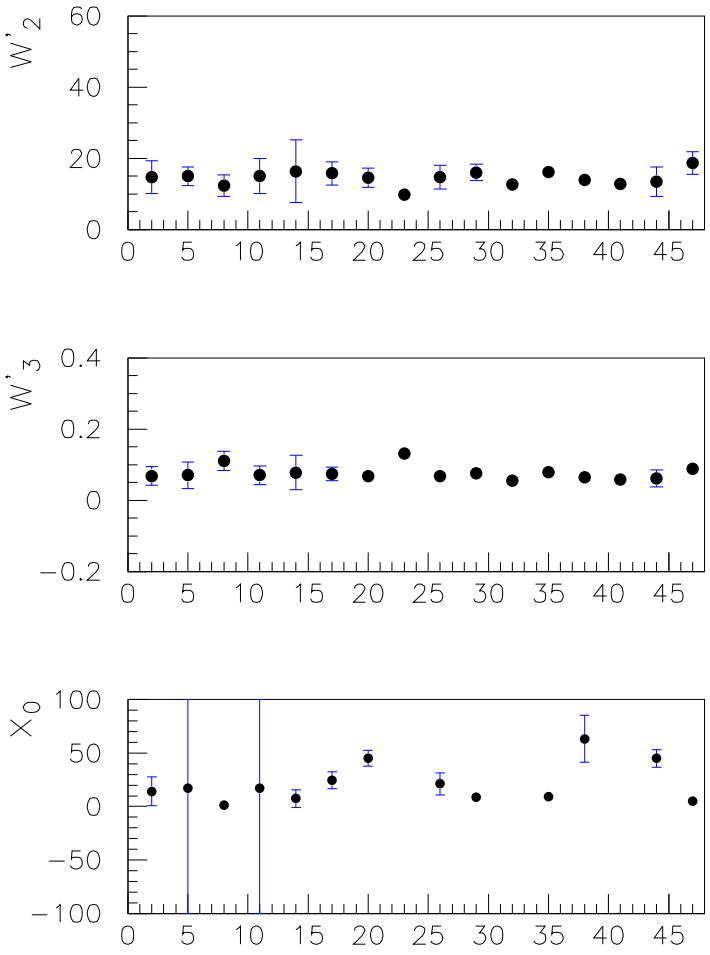

Figure 5: The fit parameters using Eq. (8) and w_2 and w_3 data versus scintillator number (left PMTs). The average values of these parameters are used in implementing the correlation function between w_2 and w_3 for the entire scintillator system.

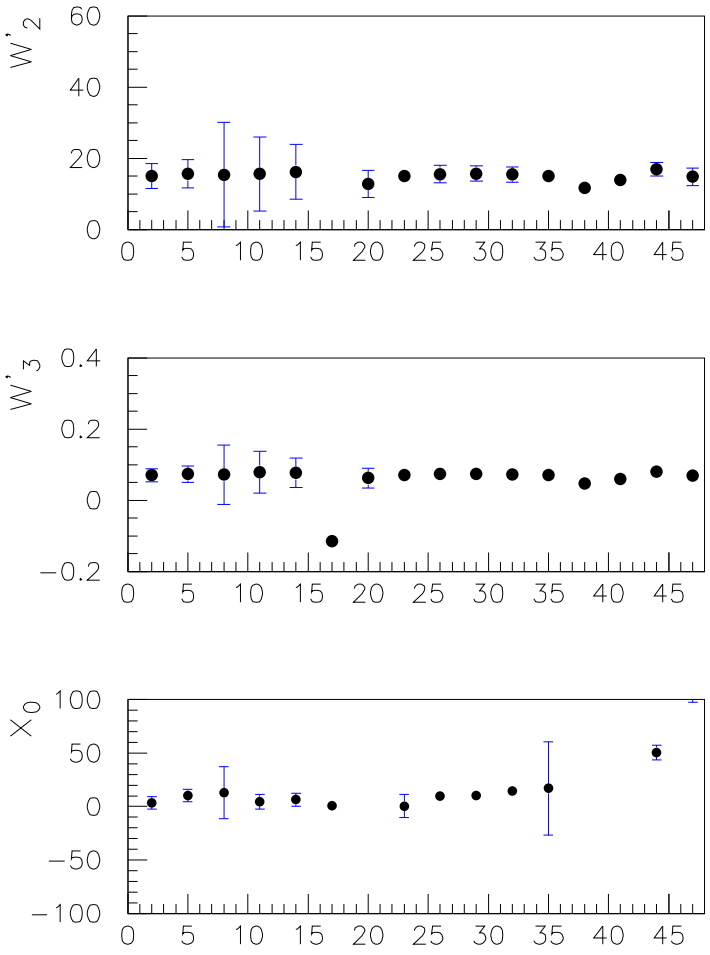

Figure 6: The fit parameters using Eq. (8) and w_2 and w_3 data versus scintillator number (right PMTs). The average values of these parameters are used in implementing the correlation function between w_2 and w_3 for the entire scintillator system.

Fig. 10).

The correlation between w_2 and w_3 in the function in Eq. (4) and (5) helps to understand the behavior of the fit and acceptable ranges for the fitted parameters. For example, the large fluctuations of the parameter w_0 are reduced using the constrained fit when compared to the fit that allows all four parameters to vary.

6 Update to the CLAS Calibration

To see the impact of these changes on the time resolution of the TOF system, we have compared the timing resolution for run 30921 using the 3 and 4 parameter time-walk functions. For the comparison we used the paddle-to-paddle calibration for run 30921 from the e1-6 run period. This is illustrated in Figs. 11, 12 and 13. The RF offsets and resolution are compared for each paddle of TOF system. The results show slightly larger delays relative to previous calibrations (using the 4-parameter function), but they are still typically less than 100 ps. The computed resolution is similar within errors to the previous parameterization, although in some cases (usually poor performing counters) at large angles it is difficult to draw any strong conclusions. We conclude that the 3-parameter function results in similar time resolution, but offers a more robust parameterization so is preferable.

We remark on the implementation of this new parameterization in the CLAS TOF calibration system. The analysis software uses Eq. (4) and (5) for time-walk corrections. This is unchanged at present. We simply use the constraint in Eq. (8) during the laser calibration procedure to determine the set of parameters, which in this case will determine $w_2 = g(w_3; w_2', w_3', x_0)$. Nevertheless all parameters w_0, w_1, w_2 and w_3 continue to be stored in the data base and used together with Eq. (4) and (5). The "3-parameter" time-walk function still uses w_0, w_1, w_2 and w_3 but w_2 is not independent of w_3. Therefore, nothing changes as far as the use of time-walk

function. [1]

References

[1] T.J. Paulus, IEEE Transactions on Nucl. Sci., NS-32, 1242 (1985).

[2] J.S. Brown *et.al.*, Nucl. Inst. and Meth. A221, 503 (1984).

[3] T. Dreyer *et.al.*, Nucl. Inst. and Meth. A309, 184 (1991).

[4] S. Banerjee *et.al.*, Nucl. Inst. and Meth. A269, 121 (1988).

[5] E.S. Smith *et.al.*, Nucl. Inst. and Meth. A432, 265 (1999).

[6] K. Kim *et.al.*, " Operation of the TOF laser Calibration System ", CLAS-NOTE 2001-004, February 2001.

[7] CLAS TOF Group, "Calibration of the CLAS TOF System", CLAS-NOTE 90-011, November 1999.

[1] The only modifications are in the calibration programs: min-main.f, min-walk.f, time-walk.f and hscan.f.

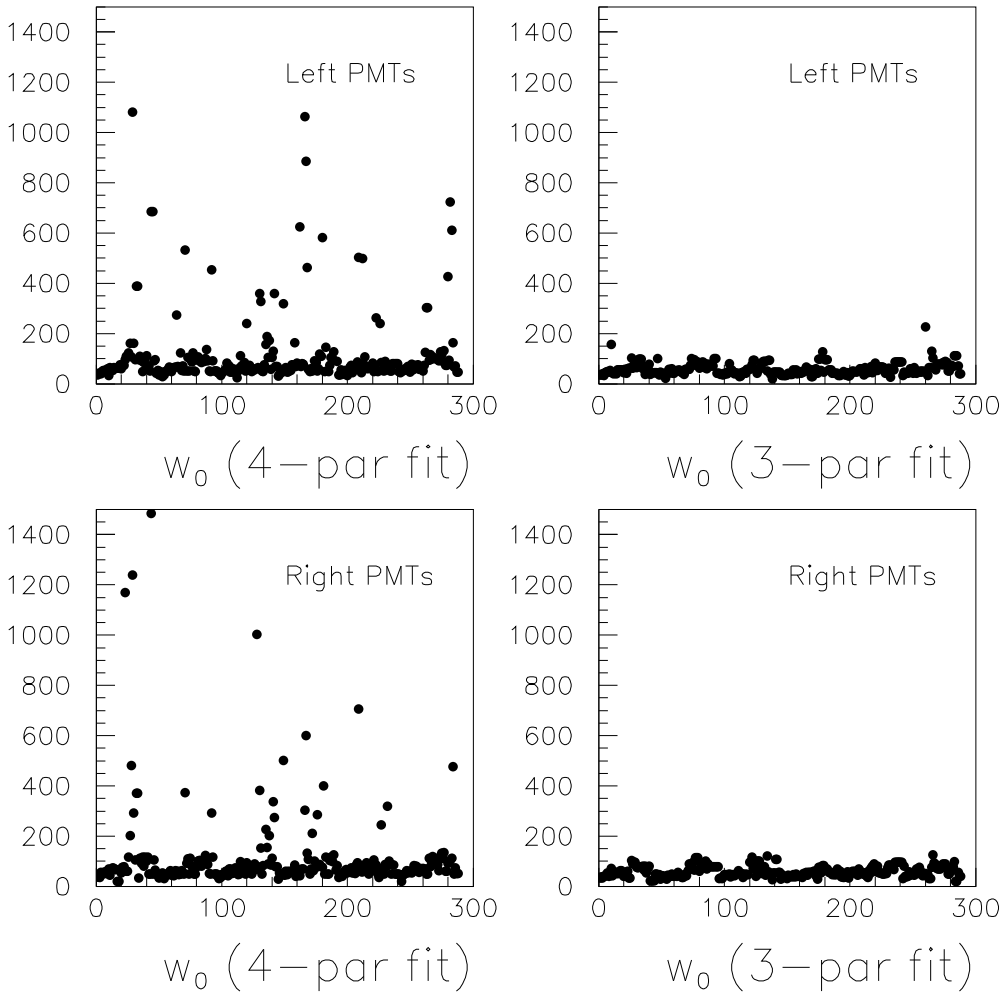

Figure 7: Fitted values of w_0. The plots on the left are from fits that allow w_2 to vary, while the plots on the right are from fits that incorporate Eq. (8) as a constraint $w_2 = g(w_3; w_2', w_3', x_0)$.

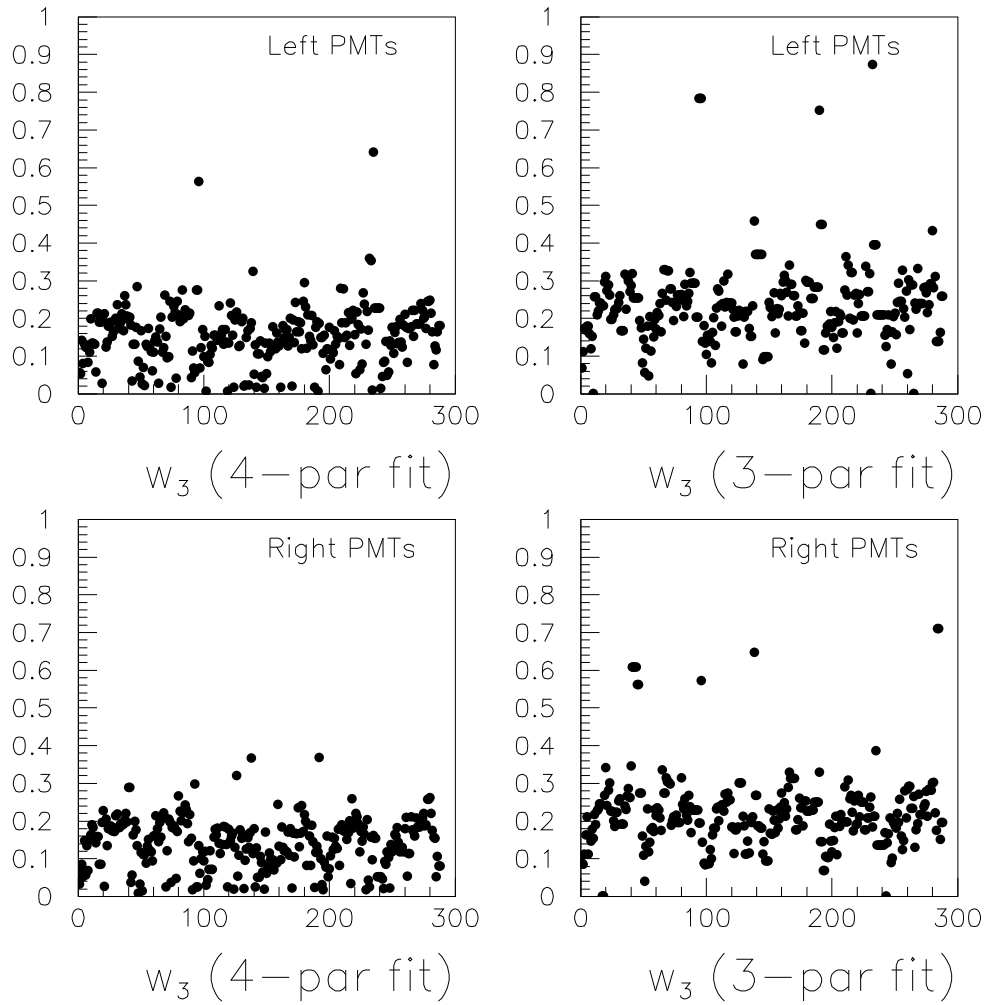

Figure 8: Fitted values of w_3. The plots on the left are from fits that allow w_2 to vary, while the plots on the right are from fits that incorporate Eq. (8) as a constraint $w_2 = g(w_3; w_2', w_3', x_0)$.

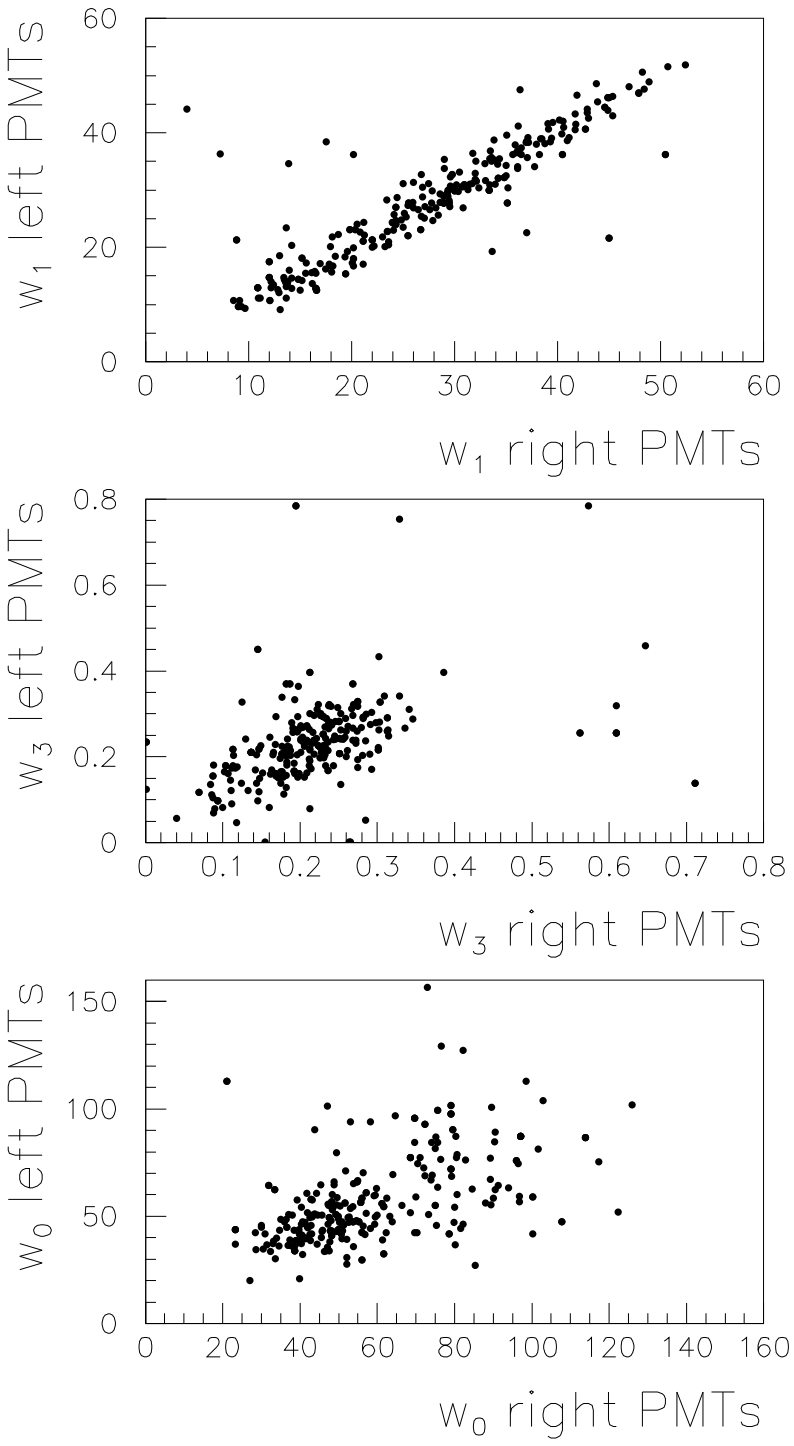

Figure 9: Fit parameters, left PMTs versus right PMTs, for fits that incorporate Eq. (8) as a constraint.

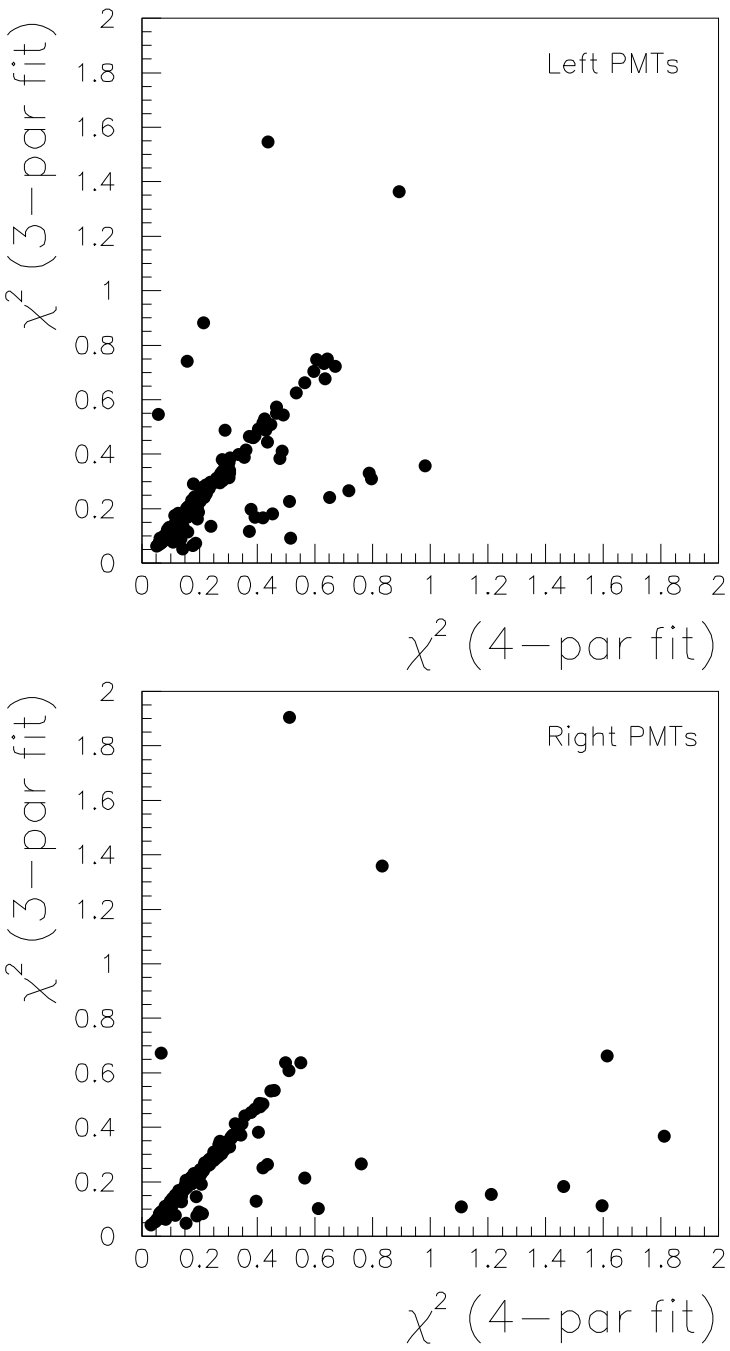

Figure 10: χ^2 of the fit with three-parameter function versus the χ^2 of the fit for the four-parameter function (no constraint) for left(top) and right(bottom) PMTs.

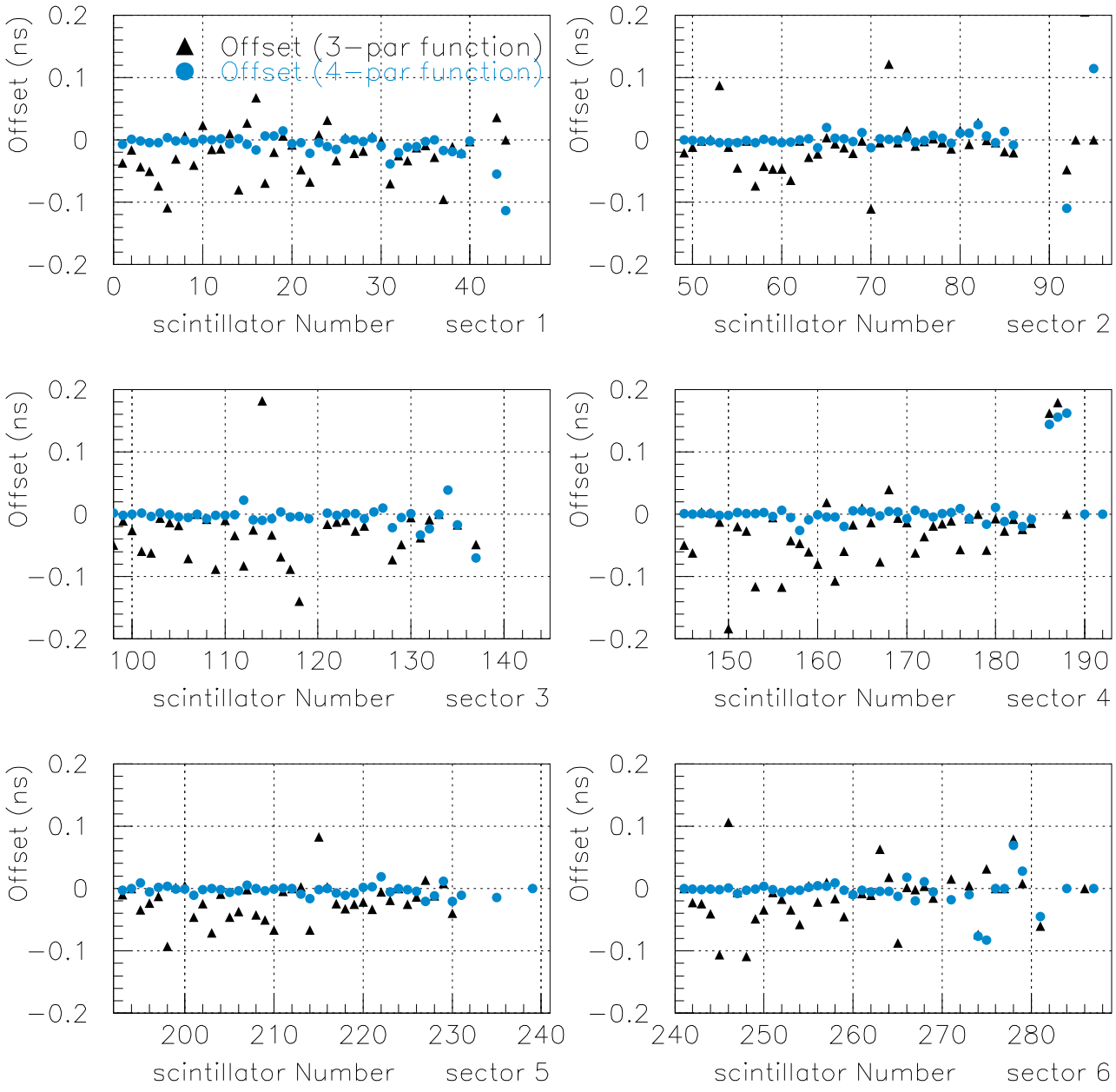

Figure 11: Comparison of paddle-to-paddle RF time offsets obtained using the 3 and 4 parameter functions relative to offsets in the data base for sectors 1 to 6 for run 30921 during the e1-6 run period.

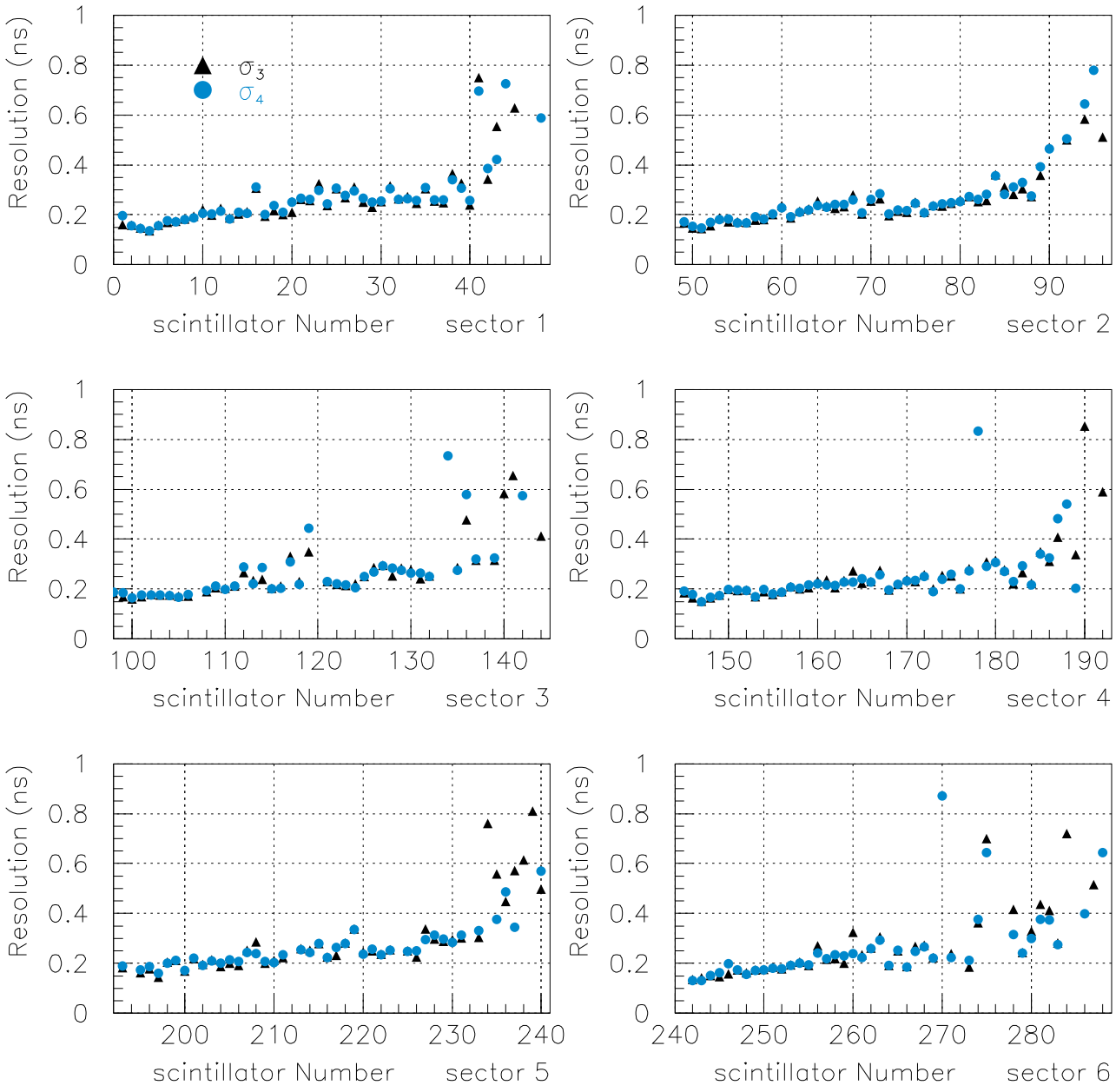

Figure 12: Comparison of paddle-to-paddle RF time resolution σ_3 and σ_4, using the 3 and 4 parameter functions respectively, for sectors 1 to 6 for run 30921 during the E1-6 run period.

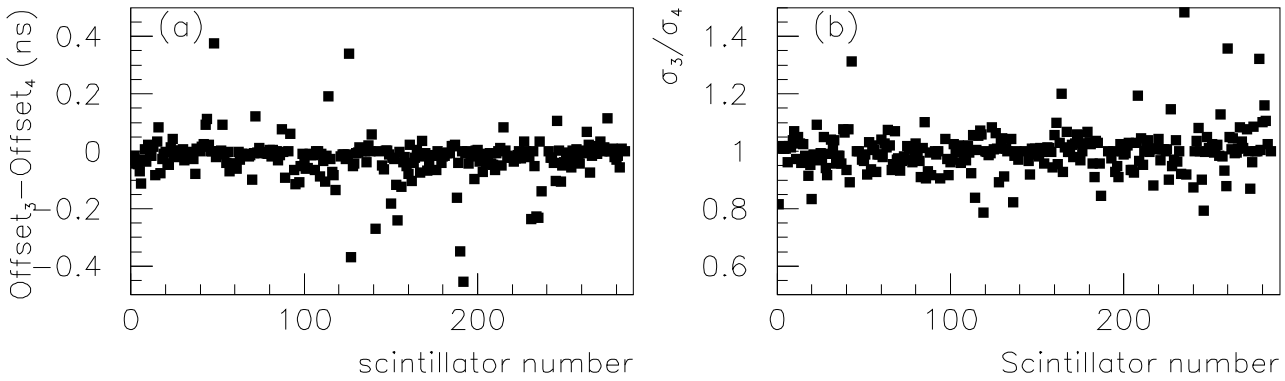

Figure 13: a) Difference of time offsets determined using the 3 and 4 parameter time-walk functions. b) Ratio of the time resolution σ_3 obtained using the 3-parameter time-walk function to the resolution σ_4 obtained using 4-parameters.